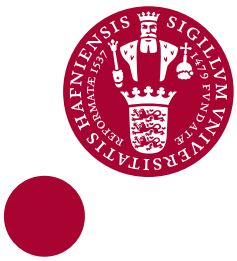

Proteomic analysis of the purple sulfur bacterium Candidatus "Thiodictyon syntrophicum" strain Cad16T isolated from Lake Cadagno

Storelli, Nicola; Saad, Maged M.; Frigaard, Niels-Ulrik; Perret, Xavier; Tonolla, Mauro

Published in:
EuPA Open Proteomics

DOI:
10.1016/j.euprot.2013.11.010

Publication date:
2014

Document version
Publisher's PDF, also known as Version of record

Available online at www.sciencedirect.com

ScienceDirect

journal homepage: http://www.elsevier.com/locate/euprot

Proteomic analysis of the purple sulfur bacterium *Candidatus* "Thiodictyon syntrophicum" strain Cad16^T isolated from Lake Cadagno

Nicola Storelli[a,b,*], *Maged M. Saad*[a], *Niels-Ulrik Frigaard*[c], *Xavier Perret*[a], *Mauro Tonolla*[a,b,d]

[a] *University of Geneva, Sciences III, Department of Botany and Plant Biology, Microbiology Unit, 30 quai Ernest-Ansermet, CH-1211 Geneva 4, Switzerland*

[b] *Laboratory of Applied Microbiology, via Mirasole 22a, CH-6500 Bellinzona, Switzerland*

[c] *Section for Marine Biology, Department of Biology, University of Copenhagen, DK-3000 Helsingør, Denmark*

[d] *Alpine Biology Center (ABC), Foundation Piora Valley, CH-6777 Quinto, Switzerland*

ARTICLE INFO

Article history:
Received 14 August 2013
Received in revised form
23 October 2013
Accepted 15 November 2013

Keywords:
Phototrophic sulfur bacteria
Dark CO_2 assimilation
Granules of poly(3-hydroxybutyrate) (PHB)
Dicarboxylate/4-hydroxybutyrate (DC/HB) cycle

ABSTRACT

Lake Cadagno is characterised by a compact chemocline with high concentrations of purple sulfur bacteria (PSB). 2D-DIGE was used to monitor the global changes in the proteome of *Candidatus* "Thiodictyon syntrophicum" strain Cad16^T both in the presence and absence of light. This study aimed to disclose details regarding the dark CO_2 assimilation of the PSB, as this mechanism is often observed but is not yet sufficiently understood. Our results showed the presence of 17 protein spots that were more abundant in the dark, including three enzymes that could be part of the autotrophic dicarboxylate/4-hydroxybutyrate cycle, normally observed in archaea.

1. Introduction

Lake Cadagno is a crenogenic meromictic lake located in the Piora valley at 1921 m above sea level in the southern Swiss Alps (46°33′ N, 8°43′ E). This lake is characterised by a narrow chemocline found at a depth of approximately 12 m that contains high concentrations of sulfates; steep gradients of oxygen, sulfide, and light; and a turbidity maximum that correlates with a dense community of phototrophic sulfur bacteria (10^7 cells ml^{-1}) [1–3]. This community is composed of species belonging to two distinct groups: the purple sulfur bacteria (PSB; family Chromatiaceae) and the green sulfur bacteria (GSB; family Chlorobiaceae) [4]. Although both groups oxidise sulfur compounds for anoxygenic photosynthesis, they also exhibit three major structural and/or metabolic

* *Corresponding author at*: Via Mirasole 22a, CH-6500 Bellinzona, Switzerland. Tel.: +41 91 814 60 12; fax: +41 91 814 60 39.
E-mail addresses: nicola.storelli@ti.ch, Nicola.Storelli@etu.unige.ch (N. Storelli).

2212-9685
http://dx.doi.org/10.1016/j.euprot.2013.11.010

differences [5]. First (1) the pigments composition (BChl and carotenoids) that allows a different structure of the light-harvesting antenna and a different type of photosynthetic reaction centre. In GSB pigments are organised into high structured organelles known as chlorosomes [6,7], while two light-harvesting complexes (LH1 and LH2) are observed in PSB [8]. The second main difference (2) is in the CO_2 fixation pathway, PSB normally fix CO_2 using the Calvin–Benson–Bassham cycle (CBB cycle) while all GSB use the reductive reverse tricarboxylic acid (rTCA) cycle [9,10]. The last but not the least difference (3) is in the deposition of sulfur globules inside or outside the cell, for PSB or GSB respectively [11].

Phototrophic sulfur bacteria are important for the primary production in many stratified lakes and have been observed to contribute with value as high as 80% of the total CO_2 fixation in some meromictic lakes [12]. In Lake Cadagno, the chemocline's contribution to the total primary production has been estimated to reach 40% despite its small volume (approximately 10% of the total lake volume). Interestingly, high rates of CO_2 assimilation have also been recorded in the dark [13]. However, the mechanism of dark CO_2 fixation, especially from PSB, remains largely unknown [14,15]. Recently, the rates of CO_2 assimilation of the most abundant phototrophic sulfur bacteria from the chemocline in Lake Cadagno were measured using both nano-scale secondary-ion mass spectrometry (nanoSIMS) [16] and $^{14}CO_2$ quantitative assimilation in dialysis bags [17]. According to these studies, the strongest CO_2 assimilators in the light and in the dark are populations of the large-celled PSB *Chromatium okenii* and the small-celled PSB *Candidatus* "Thiodictyon syntrophicum" respectively [18]. Moreover, the PSB *Candidatus* "T. syntrophicum" population is also a strong CO_2 assimilator in the presence of light. Although it only represents approximately 2% of the total chemocline's bacterial population, *Candidatus* "T. syntrophicum" appears to play a key role in CO_2 fixation in Lake Cadagno, both in the presence and absence of light [17].

The elucidation of cellular metabolisms in response to different environmental conditions requires the use of a combination of different techniques that can record metabolic adaptations under different environmental conditions. Comparative proteomics allows a global analysis of differentially expressed functional and regulatory protein [19–23]. Two-dimensional polyacrylamide gel electrophoresis (2D-PAGE) is generally applied for separating large numbers of proteins and measuring their differential expression levels by comparing spot intensities [24,25]. Two-dimensional difference gel electrophoresis (2D-DIGE) has been implemented as a powerful alternative to conventional 2D-PAGE for quantitative expression analysis [26,27]. Proteins from 2D-PAGE or 2D-DIGE are commonly identified by peptide mass fingerprinting (PMF) using matrix-assisted laser desorption ionisation-time-of-flight mass spectrometry (MALDI-TOF MS) [28,29].

The major aim of this study was to elucidate the CO_2 assimilation processes of the PSB *Candidatus* "Thiodictyon syntrophicum" strain Cad16^T in light and especially in the dark by proteomic analysis. The total proteins were extracted in the light and in the dark from bacterial suspensions that were incubated with a photoperiod of 12 h of light followed by 12 h of dark during approximately 10 days. Sample extracts from the light and dark were compared using 2D-DIGE followed by MALDI-TOF mass spectrometry identification using the 7,3-Mbp draft genome of strain Cad16^T as database.

2. Materials and methods

2.1. Media and growth conditions

Candidatus "T. syntrophicum" strain Cad16^T [18] was grown in Pfennig's Medium I [30]: 0.25 g of KH_2PO_4 l^{-1}, 0.34 g of NH_4Cl l^{-1}, 0.5 g of $MgSO_4{\cdot}7H_2O$ l^{-1}, 0.25 g of $CaCl_2{\cdot}2H_2O$ l^{-1}, 0.34 g of KCl l^{-1}, 1.5 g of $NaHCO_3$ l^{-1}, 0.02 mg of vitamin B_{12} l^{-1} and 0.5 ml of trace element solution SL12 l^{-1}. The medium was prepared in 2 l bottles using a flushing gas composed of 80% N_2 and 20% CO_2 according to Widdel and Bak [31] and was reduced by the addition of 1.10 mM $Na_2S{\cdot}9H_2O$ and adjusted to a pH of approximately 7.0. Cultures were incubated at room temperature (20–23 °C) and subjected to cycles of 12 h of light followed from 12 h of dark until the cultures reach the density of approximately 10^7 cells per ml^{-1} (about 10 days). The light intensity was set up at 6 μE m^{-2} s^{-1} generated with incandescent 60 W bulbs. Bacterial growth was followed by measuring the optical density of culture aliquots at 650 nm using a UV/VIS Spectrometer Lambda 2S (Perkin-Elmer Inc, Waltham, MA, USA). Concentrations of sulfide in the cultures were measured daily and adjusted to about 1.00 mM throughout the experiments.

The differential protein expressions of *Candidatus* "T. syntrophicum" strain Cad16^T at autotrophic growth conditions in the light and in the dark were investigated. How say above, bacterial cells were exposed to a photoperiod of 12 h of light (07:00–19:00) followed by 12 h of dark (19:00–07:00) for approximately 10 days until they reached an optical density of approximately $OD_{650} = 0.6$ corresponding to approximately 10^7 cells per ml^{-1}. Then, the total proteins were extracted after 4 h of light (at 11:00) and again 12 h later after 4 h of dark (at 23:00) always following the cycles of light and dark of 12 h each. Three independent cultures were used to ensure the biological reproducibility of the experiment, and prior to the 2D-DIGE experiment, each protein extract was previously analysed on silver-stained 2-DE gels in triplicate.

2.2. Total cell count

Cell concentrations of pure bacterial cultures were determined using samples fixed with 4% formaldehyde (final concentration) and stained with 0.001% (w/v) 4′,6-diamidino-2-phenylindole (DAPI) (final concentration). Ten μl of each fixed and stained sample were deposited onto polycarbonate filters as described in Hobbie et al. [32] and observed at 100-fold magnification using an epifluorescence microscope (Axiolab, Zeiss Germany) and the filter set F31 (Zeiss, Germany). Twenty fields of 0.01 mm^2 were counted, and cell densities were expressed as the mean number of cells ml^{-1} (±standard error).

2.3. Protein extraction

The total proteins were extracted from cells from exponentially growing cultures with an OD_{650} of ca. 0.6, which corresponds to approximately 1.0×10^7 cells per ml^{-1}. The

Table 1 – CyDye labelling scheme and gel setup for 2D-DiGE analysis.

Gel #	CyDye	Sample type
1	Cy3	Light 1 (50 μg)
	Cy5	Dark 1 (50 μg)
	Cy2	Internal standard (50 μg)
2	Cy3	Dark 1 (50 μg)
	Cy5	Light 1 (50 μg)
	Cy2	Internal standard (50 μg)
3	Cy3	Light 2 (50 μg)
	Cy5	Dark 2 (50 μg)
	Cy2	Internal standard (50 μg)
4	Cy3	Dark 2 (50 μg)
	Cy5	Light 2 (50 μg)
	Cy2	Internal standard (50 μg)
5	Cy3	Light 3 (50 μg)
	Cy5	Dark 3 (50 μg)
	Cy2	Internal standard (50 μg)
6	Cy3	Dark 3 (50 μg)
	Cy5	Light 3 (50 μg)
	Cy2	Internal standard (50 μg)

liquid bacterial cultures (500 ml) were centrifuged for 15 min at 15,000 × *g*, and the pellets were washed thrice with PBS 1× and twice with 0.5 M Tris–HCl, pH 6.8. The washed pellets were resuspended in 2 ml of lysis buffer (7 M urea, 2 M thiourea, 30 mM Tris–HCl, pH 8.6, 4% (w/v) CHAPS) and were incubated overnight at −20 °C. The samples were sonicated (SONOPULS HD 2070, Bandelin Electronics, Germany) for 5 cycles of 15 s each at 25% of the maximal power, with a pause of 5 min on ice between each cycle, and then centrifuged for 15 min at 20,000 × *g* at 4 °C. The supernatants were washed twice with acetone for 60 min at −20 °C to eliminate all pigments that could interfere with the dyes during the 2D-DIGE experiment. After centrifugation for 10 min at 15,000 × *g*, the protein concentrations present in the pigment-free supernatants were measured by Bradford assays (Bio-Rad, Reinach BL, Switzerland) according to the manufacturer's instructions [33]. The samples were then aliquoted into 50 μg portions and stored at −80 °C.

2.4. *2D-DIGE analysis*

The protein extracts were labelled with Cy2, Cy3 and Cy5 CyDye DIGE Fluor minimal dyes (GE Healthcare Bio-Sciences AB, Uppsala, Sweden) for 30 min in the dark according to the manufacturer's instructions for the labelling process (8 pmol per 50 μg^{-1}). In brief, 50 μg of protein from light or dark conditions of three independent biological replica were individually labelled using 400 pmol of either Cy3 or Cy5. A mixed (equal pool of all samples, 3× light and 3× dark) internal standard labelled with 400 pmol of Cy2 was included for spot normalisation and to allow comparison across all gels within the analysis as published previously [27,34]. On completion of the labelling reaction, the Cy3 and Cy5 labelled samples were combined pair wise and 50 μg of Cy2-labelled internal standard was added to each gel (see Table 1), as recommended by the manufacturer.

Each combined labelled sample (150 μg of protein) was resuspended in solubilisation buffer (SB: 7 M urea, 2 M thiourea, 30 mM Tris–HCl pH 8.5, 4% (w/v) CHAPS, 40 mM DTT, 1% (v/v) 3–10 NL IPG buffer, 0.002% (w/v) bromophenol blue) prior to isoelectric focusing (IEF). IEF separation, was performed in 24 cm DryStrips with a nonlinear pH 3–10 gradient (GE Healthcare Bio-Sciences AB, Uppsala, Sweden). The PlusOne DryStrip Cover fluid was used to fill the 24 cm ceramic holders (GE Healthcare Bio-Sciences AB, Uppsala, Sweden) containing the DryStrips, which were then introduced into an Ettan®IPGphor 3 (GE Healthcare Bio-Sciences AB, Uppsala, Sweden). After 18 h of strip rehydration at 18 °C, the IEF programme was performed at 18 °C under the following steps: 300 V for 4 h, 300–1000 V gradient for 70 min, 3000 V for 4 h, 3000–6000 V gradient for 2 h, 6000 V for 1 h, 6000–8000 V gradient for 2 h, and 8000 V until a total voltage of 120,000 V h was reached. The isoelectrofocused strips were incubated in equilibration solution (ES: 0.5 M Tris–HCl, pH 8.5, 6 M urea, 30% (v/v) glycerol, 2% (w/v) SDS) for 15 min with the addition of 2.0% (w/v) DTT, then for 10 min in ES with the addition of 2.5% (w/v) iodoacetamide. The second dimension of separation, SDS–PAGE, was performed in an EttanTM DALTsix Electrophoresis System (GE Healthcare Bio-Sciences AB, Uppsala, Sweden) following the manufacturer's instructions for overnight migration (80 V, 10 mA per gel). The isoelectrofocused strips were applied onto a 12% polyacrylamide gel casted in low-fluorescence glass plates for EttanTM DALT using a DALTsix Gel Caster (GE Healthcare Bio-Sciences AB, Uppsala, Sweden). Immediately after electrophoresis, the gels were scanned in an EttanTM DIGE Imager (GE Healthcare Bio-Sciences AB, Uppsala, Sweden) following the manufacturer's instructions and default parameters. The differences in the protein expression levels were analysed using the Melanie© 7.0 software [Geneva Bioinformatics (GeneBio) SA, Geneva, Switzerland]. The Cy3/Cy5 2D-DIGE image overlays were obtained for bi-fluorescence by processing the individual scanned images with ImageJ software (http://rsbweb.nih.gov/ij/).

2.5. *Proteins identification*

For protein characterisation, the 2D-DIGE gels were stained with Coomassie brilliant blue R-250 after the fluorescence image acquisition [35]. The differentially expressed protein spots were picked manually using a scalpel and digested using trypsin gold enzymes following the manufacturer's instructions (Promega AG, Dübendorf, Switzerland). A volume of 0.5 μl of each sample was loaded onto a FlexiMass™ target well, which was overlaid with 0.5 μl of a saturated α-cyano-4-hydroxycinnamic acid solution in 50% (v/v) acetonitrile, 50% (v/v) dH_2O and 0.1% (v/v) trifluoroacetic acid (TFA) and crystallised by air drying. The peptide mix PepMix1 (LaserBio Labs, Valbonne, France) was used as a standard for calibration. Peptide mass fingerprints (PMFs) of tryptic peptides were collected by an AXIMA Confidence matrix-assisted laser desorption/ionisation time-of-flight tandem mass spectrometry (MALDI-TOF-MS) (Shimadzu Biotech, Manchester, UK). Carbamidomethylation of cysteine (Cys) and oxidation of methionine (M) as fixed and variable modifications, respectively, were taken into account for database searching.

The following search parameters were used in all MASCOT searches: tolerance of one missed cleavage and a maximum error tolerance of 0.3 Da in the MS data and 0.8 Da in the MS/MS data. All peptide PMFs and peptide fragmentation fingerprints (PFFs) data were searched using MASCOT search engine (http://www.matrixscience.com; [36]) against an in-house database containing the draft genome of strain Cad16^T in addition to public databases (NCBInr and Swissprot). Identifications were accepted based on the significant MASCOT Mowse score and direct correlation between the identified protein and its estimated molecular mass and pI determined from the 2D-gel. A MASCOT score of 64 corresponds to $p < 0.05$ for mass fingerprint experiments, while a MASCOT score of 37 corresponds to $p < 0.05$ for MS/MS sequencing; these thresholds were chosen as the cutoff for a significant hit.

2.6. *Draft genome of strain Cad16^T*

The draft genome sequence of *Candidatus* 'Thiodictyon syntrophicum' strain Cad16^T was determined by pyrosequencing in the laboratory of Dr. S.C. Schuster (Z. Liu, K. Vogl, N.-U. Frigaard, L.P. Tomsho, S.C. Schuster and D.A. Bryant, unpubl. data) at the Genomics Core Facility of Pennsylvania State University. Paired-end reads from GX-20 FLX Titanium chemistries were assembled into 1352 primary contigs of a total of 7.3 Mbp. A total of 7063 ORFs were detected by annotation using a pipeline based on FGENESB software (Softberry, Inc., USA), Artemis (Sanger Institution, UK), and custom-made Perl scripts (ActivePerl; ActiveStateInc., Vancouver, BC, USA). The genome sequencing project has been assigned the bioproject number PRJNA32527 in GenBank (http://www.ncbi.nlm.nih.gov/bioproject).

2.7. *Analysis of the total mRNA during autotrophic growing conditions*

To determine a relationship between the protein spots that were analysed and their actual gene expression, the total mRNA of *Candidatus* "T. syntrophicum" strain Cad16^T was extracted and converted to cDNA prior to Solexa paired-end sequencing [37]. Transcriptome analysis was performed from the cells of strain Cad16^T that were incubated under the same conditions of growth that were applied for the proteomics analysis. The total mRNA was extracted after 4 h of light (at 11:00). The total RNA of strain Cad16^T was isolated using Trizol reagent (Invitrogen, Zug, Switzerland) and enriched for mRNA using the MicrobExpress kit (Ambion, Zug, Switzerland) following the manufacturer's instructions. Conversion to cDNA was performed using the MessageAmp IIBacteria kit (Ambion, Zug, Switzerland) and the SuperScript ds-cDNA Synthesis kit (Invitrogen, Zug, Switzerland) according to the manufacturers' instructions. The cDNA was subjected to Solexa paired-end sequencing (2 × 75 bp) of a 200-bp insert library (Beijing Genome Institute). Paired-end sequencing was used rather than single-end sequencing to increase the number of bases available for the analysis of the transcriptome.

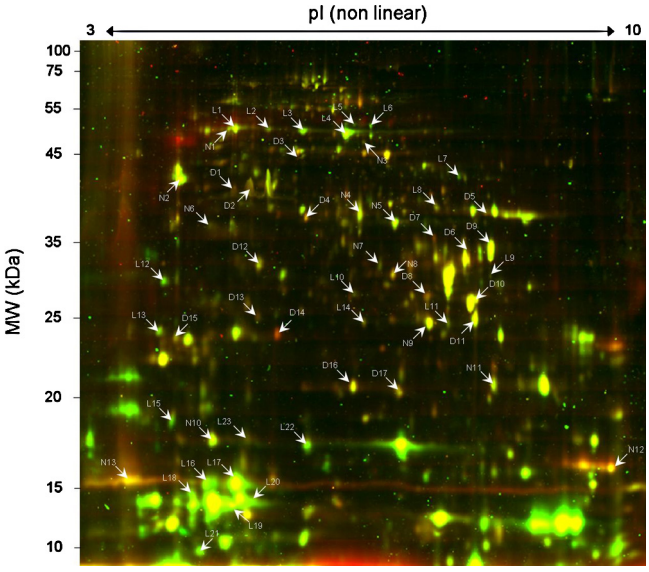

Fig. 1 – The protein expression patterns of *Candidatus* "T. syntrophicum" strain Cad16^T separated in a 24 cm, pH 3–10 nonlinear strip and a 12% polyacrylamide gel. The proteins that were extracted in the presence of light were labelled with Cy3 (green), and those extracted during the dark phase were labelled with Cy5 (red), both of which were submitted to 2D-DIGE analysis. Proteins more abundant in the light are characterised by an "L" before the number, and those in the dark are characterised by a "D". Non-regulated proteins that were present in the same quantity in both conditions are characterised by an "N" before the number. (For interpretation of the references to color in this text, the reader is referred to the web version of the article.)

3. Results and discussion

3.1. *Differentially expressed proteome analysis (2D-DIGE)*

A representative 2D-DIGE image (Table 1, gel 1) showing the fluorescent levels of the total proteins extracted in the light (Cy3, green) and in the dark (Cy5, red) is shown in Fig. 1. More than 1400 protein spots were detected during the analysis of the 2D-DIGE gel using Melanie 7.0 software. Among them, 56 protein spots had an ANOVA p-value <0.05. These protein spots were selected as showing a differential expression that was statistically significant. Considering 1.5-fold to be the minimal level of differential expression, the expression levels of 40 protein spots were modified when *Candidatus* "T. syntrophicum" strain Cad16^T was exposed to the light compared to their exposure to 4 h of darkness. Sixteen spots from the 56 protein spots showing an ANOVA p-value < 0.05 were excluded from the analysis because they were below the differential expression threshold ratio of 1.5 measured through the florescence intensity of the signal. Among the 40 differentially expressed spots satisfying the ANOVA and intensity parameters, 23 spots were more abundant in the presence of the light, and 17 spots were more abundant in the dark. The differentially expressed proteins were identified by peptide mass

Table 2 – List of proteins identified by MALDI-TOF MS/MS.

Spot number as given on the 2-D gel images	Ordered Locus Names of the best match of Cad16T genome	Protein encoded by the best matching gene in Cad16T genome	Experimental Molecular weight (Mw) inducted by kDa	Isoelectric Point (pI)	Number of matching peptides used for Mascot searches	% of sequence coverage of the PMF match	Anova *P*	Fold Expression (positive light; negative dark)*	Number of Reads Mapping to Gene (mRNA)
L1	Thd3346	50S ribosomal protein L28	58,149	5.19	26	36	0.0017	4.91	2157
L2	Thd6617	NADPH-dependent glutamate synthase beta chain and related oxidoreductases	60,153	5.37	15	25	0.0008	5.73	1038
L3	Thd3787	Outer membrane protein (porin)	69,523	6.02	15	38	0.0004	5.10	4340
L4	Thd3932	ATP synthase subunit alpha	55,095	5.41	10	23	0.0006	1.69	1636
L5	Thd3787	Outer membrane protein (porin)	69,523	6.02	12	34	0.0003	3.84	4340
L6	Thd2499	Outer membrane protein/protective antigen OMA87	86,955	6.61	20	23	0.0005	2.68	462
L7	Thd5879	Transcription termination factor Rho	45,458	6.76	10	24	0.0070	1.53	119
L8	Thd6580	Poly(R)-hydroxyalkanoic acid synthase subunit PhaE	40,707	7.86	20	36	0.0090	1.92	661
L9	Thd4312	Uncharacterised conserved protein (no conservative domain)	21,660	9.35	6	19	0.0230	1.96	666
L10	gi|390,952,282	Amino acid ABC transporter substrate-binding protein (Thiocystis violascens DSM 198)	33,657	6.32	7	25	0.0074	1.59	x***
L11	Thd5116	ABC-type molybdate transport system, periplasmic component	26,330	8.63	3 (PFF)**	11	0.0007	3.10	53
L12	Thd5760	Uncharacterised protein conserved in bacteria (tellurite res. TerB)	17,976	4.77	7	42	0.0065	2.83	912
L13	Thd5501	Hypothetical protein (no conservative domain)	19,319	6.85	9	37	0.0197	1.58	1376
L14	Thd2504	Ribosome recycling factor (RRF)	19,442	5.86	9	43	0.0003	5.66	178
L15	Thd0032	Elongation factor G (EF-G) family	17,738	4.86	6	29	0.0135	2.30	3755
L16	Thd3751	Hypothetical protein (no conservative domain)	9907	4.76	4	34	0.0500	2.44	2094

– Table 2 (*Continued*)

Spot number as given on the 2-D gel images	Ordered Locus Names of the best match of Cad16T genome	Protein encoded by the best matching gene in Cad16T genome	Experimental Molecular weight (Mw) inducted by kDa	Isoelectric Point (pI)	Number of matching peptides used for Mascot searches	% of sequence coverage of the PMF match	Anova P	Fold Expression (positive light; negative dark)*	Number of Reads Mapping to Gene (mRNA)
L17	Thd6554	phasin (PhaP)	15,774	5.15	12	71	0.0162	2.77	2163
L18	Thd6554	phasin (PhaP)	15,774	5.15	12	63	0.0229	2.47	2163
L19	Thd4286	hypothetical protein (SpoVT/AbrB like domain)	8373	6.18	5	73	0.0450	2.49	1095
L20	Thd2631	Dissimilatory sulfite reductase (desulfoviridin), gamma subunit (DsrC/TusE)	12,680	5.13	1 (PFF)**	11	0.0110	2.01	694
L21	Thd4540	Co-chaperonin GroES (HSP10)	10,520	5.16	9	84	0.0205	1.83	118
L22	Thd6562	Methyl-accepting chemotaxis protein	20,832	7.71	10	38	0.0090	2.39	1357
L23	Thd4906	Molecular chaperone (small heat shock protein) Hsp20	17,812	5.34	9	47	0.0006	4.42	3019
D1	Thd2748	Parvulin-like peptidyl-prolyl isomerase	27,831	5.20	16	63	0.0128	−2.05	1645
D2	Thd2748	Parvulin-like peptidyl-prolyl isomerase	27,831	5.20	18	58	0.0007	−4.22	1645
D3	Thd1984	Hypothetical protein (no conservative domain)	53,964	5.91	13	27	0.0027	−3.88	49
D4	Thd4019	Maltose-binding periplasmic proteins/domains (MalE)	42,270	5.74	15	39	0.0138	−1.88	84
D5	Thd6555	Acetyl-CoA acetyltransferase	40,614	7.02	15	38	0.0144	−1.80	488
D6	Thd5260	Malate/lactate dehydrogenases	35,171	7.10	12	38	0.0350	−2.24	546
D7	Thd6937	Hypothetical protein (no conservative domain)	19,781	5.31	12	72	0.0256	−1.85	67
D8	Thd1849	Parvulin-like peptidyl-prolyl isomerase	26,932	6.45	12	58	0.0070	−2.20	96
D9	Thd0849	Parvulin-like peptidyl-prolyl isomerase	33,930	8.37	11	40	0.0009	−3.34	575
D10	Thd6937	Hypothetical protein (no conservative domain)	19,781	5.31	13	72	0.0004	−2.81	67
D11	Thd0844	3-hydroxyacyl-CoA dehydrogenase	28,025	6.75	12	54	0.0396	−1.85	201

– Table 2 (*Continued*)

Spot number as given on the 2-D gel images	Ordered Locus Names of the best match of Cad16T genome	Protein encoded by the best matching gene in Cad16T genome	Experimental Molecular weight (Mw) inducted by kDa	Isoelectric Point (pI)	Number of matching peptides used for Mascot searches	% of sequence coverage of the PMF match	Anova *P*	Fold Expression (positive light; negative dark)*	Number of Reads Mapping to Gene (mRNA)
D12	Thd3915	Parvulin-like peptidyl-prolyl isomerase	36,171	6.07	15	43	0.0007	−2.85	285
D13	Thd1338	Peroxiredoxin	27,023	5.28	13	56	0.0036	−2.75	411
D14	Thd0914	Peroxiredoxin	24,285	5.50	11	53	0.0010	−2.12	575
D15	Thd2858	Uncharacterised protein conserved in bacteria (tellurite res. TerB)	25,972	4.85	1 (PFF)**	4	0.0201	−2.07	74
D16	Thd2672	Superoxide dismutase, manganese-dependent	21,228	5.81	3 (PFF)**	19	0.0067	−2.13	301
D17	Thd4647	Hypothetical protein (no conservative domain)	22,294	7.98	16	70	0.0040	−3.34	124
N1	Thd5863	Periplasmic glucans biosynthesis protein	59,079	5.22	11	23	0.7305	0.93	167
N2	Thd0697	Enolase	45,200	4.80	22	50	0.1278	−0.47	519
N3	Thd5907	Ribulose 1,5-bisphosphate carboxylase, large subunit (CbbM)	51,271	5.87	19	43	0.1757	−0.18	28
N4	Thd6175	Fructose/tagatose bisphosphate aldolase	38,472	5.83	16	43	0.4588	0.90	422
N5	Thd6763	Spermidine/putrescine-binding periplasmic protein	39,817	6.51	11	44	0.9825	1.01	171
N6	Thd4648	Gluconolactonase	38,924	5.14	8	23	0.1500	−0.60	106
N7	Thd1255	Phosphoribulokinase	33,289	5.89	15	48	0.1635	−0.59	34
N8	Thd1255	Phosphoribulokinase	33,289	5.89	12	41	0.5560	−0.56	278
N9	Thd0660	Superoxide dismutase, manganese-dependent	22,142	6.47	4** (PFF)	24	0.7871	0.96	408
N10	Thd2537	Peroxiredoxin	17,358	5.05	8	58	0.2339	−0.55	1966
N11	Thd2730	Predicted 6-phosphogluconate dehydrogenase	36,268	5.48	7	28	0.2910	−0.74	44
N12	Thd5951	Ribosomal protein L9	15,334	9.10	9	45	0.1741	0.51	522
N13	Thd6339	Ribosomal protein L7/L12	12,979	4.67	5	54	0.1247	−0.33	6534

List of proteins identified by MALDI-TOF MS/MS *Candidatus* "Thiodictyon syntrophicum" strain Cad16^T proteins from minimal autotrophic medium (Pfennig's medium) after 4 h of light (11:00 = L1-22) and after 4 h of dark (23:00 = D1-18) in a continuos photoperiod of 12 h of light fallowed by 12 h of dark (7:00–19:00) light/dark mean ANOVA < 0.05 and 1.5 fold expration.

* Average ratio of the protein fold expression (abundance) between total cellular proteins isolated from Light (L) vs. Dark (D), The minimal level of differential expression was selected >1.5-fold with *P* value < 0.05. Proteins that have fold expression 01.5 are considered as stable proteins (N).

** Proteins identified by PFF with one or more independent peaks of the PMF spectrum.

*** Proteins not presents in the trascritome analysis report.

fingerprinting (PMF) or peptide fragmentation fingerprinting (PFF) (Table 2). The reliability of the protein identification was assessed on the basis of Mascot scores (p-value < 0.05) using the draft genome of strain Cad16^T as a reference database (in-house database).

The transcriptome isolated from strain Cad16^T in the light was used to confirm the expression of the analysed protein spots (Table 2; right column: *Number of Reads Mapping to Gene (mRNA)*).

3.2. *Protein spots more abundant in the presence of light*

Among the 23 spots that were more abundant in the presence of light, we found proteins that were predominantly involved with (a) protein biosynthesis, (b) storage biosynthesis, (c) sulfur compound oxidation and photosynthesis (d), trans-membrane transport and (e) other metabolic processes.

3.2.1. *Protein biosynthesis*

During the light phase, strain Cad16^T over-expressed many proteins involved in protein biosynthesis, such as ribosomal proteins and enzymes needed for gene transcription (Table 2, spots L1, L7, L14, L15, L21 and L23). The transcription of genes, performed by RNA polymerase, is ended by the transcription terminator factor Rho (Table 2, spot L7), which binds to the transcription terminator pause site and stops mRNA transcription [38]. The ribosome links the amino acids and translates the genes found on the mRNA into proteins. In prokaryotes, the ribosome is composed of two subunits of 50S and 30S. The large subunit catalyses peptide bond formation [39]. The ribosome of *Escherichia coli* contains 22 proteins in the small subunit, labelled S1–S22, and 36 proteins in the large subunit, labelled L1–L36 [40]. In this study, L28 showed an up-regulation during the light period (Table 2, spot L1). During the translational step, the ribosome interacts with different GTPase factors as well as initiation factors (IFs), elongation factors (EFs) and release factors (RFs) via its conserved C-terminal domain [41]. Initiation factors IF1, IF2 and IF3 are involved in the initiation of protein synthesis to form the 70S initiation complex. Elongation factors EF-Tu, EF-Ts and EF-G (Table 2, spot L15) are needed for the extension of protein synthesis. Release factors RF1, RF2 and RF3 regulate the steps during the termination phase of translation. Lastly, ribosome recycling factor (RRF) (Table 2, spot L14), along with EF-G, catalyses the recycling of the ribosomal subunits [42].

The efficient folding of many newly synthesised proteins depends on assistance from molecular chaperones. Molecular chaperones, such as the heat shock proteins (HSPs), are among the more abundant cytosolic proteins found in cells from the three kingdoms: eukaryotes, bacteria and archaea. Their role is to recognise and bind nascent polypeptide chains and partially folded protein intermediates, preventing their aggregation and misfolding, both under normal conditions and when cells are exposed to stresses such as high temperature [43]. Protein spots L21 and L23 (Table 2), which were more abundant under the light conditions, corresponded to chaperones HSP10 and HSP20, respectively.

The large number of proteins involved in protein biosynthesis, storage mechanisms (see Section 3.2.2 below), and photosynthesis (see Section 3.2.3 below) suggested a cell state characterised by an active metabolism in the presence of a relatively high content of nutrients and energy, which could be used for protein biosynthesis during cell growth. The increased expression of the enzyme NADPH-dependent glutamate synthase beta chain (Table 2, spot L2), which is responsible for the production of amino acids, confirmed the high energetic state of the cells by promoting the turnover of NAD(P)H that originated from photosynthesis.

3.2.2. *Storage biosynthesis*

Interestingly, 3 proteins (Table 2, spots L8, L17 and L18) involved in a storage mechanism that produces intracellular granules of polyhydroxyalkanoates (PHAs) were over-expressed under the light conditions. This mechanism has been observed in a wide variety of microbes that accumulate PHAs as a carbon and energy storage reserve when essential nutrients, such as nitrogen or phosphorus, are limited but carbon sources are in excess [44,45]. A typical PHA that is accumulated in microbial cells is poly(3-hydroxybutyrate) (PHB), which consists of 1000–30,000 hydroxy fatty acid monomers, forming a granule in the cytoplasm. PHB synthesis in *Alcaligenes eutrophus* is stimulated by both high intracellular concentrations of NAD(P)H and high ratios of NAD(P)H/NAD(P)$^+$ which also inhibit citrate synthase activity and thereby facilitating the metabolic flux of acetyl-CoA to the PHB synthetic pathway [46]. The most important enzyme in the biosynthesis of this storage substance is the PHA synthase. PHA synthases currently are divided into four classes depending on their subunit composition and substrate specificity. It has been shown in other species of PSB, such as *Allochromatium vinosum* and *Thiocystis violacea* [47,48], that the presence of a Class III PHA synthase consists of two subunits (PhaC and PhaE). This enzyme is responsible for the final step of the synthesis, in which PHB is synthesised from (R)-3-hydroxybutyryl-CoA molecules and free CoA is released. However, the process typically starts from 2 acetyl-CoA molecules that are coupled together to form acetoacetyl-CoA in a condensation reaction that is catalysed by 3-ketothiolase (PhaA), and this product is subsequently stereoselectively reduced to (R)-3-hydroxybutyryl-CoA in a reaction catalysed by NADPH-dependent acetoacetyl-CoA reductase (PhaB). However, PHB can also be synthesised from an intermediate of the beta-oxidation/bio-synthesis of fatty acids. The molecule of trans-2-enoyl-CoA is converted to (R)-3-hydroxyacyl-CoA via (R)-specific hydration, which is catalysed by (R)-specific enoyl-CoA hydratase (PhaJ) [49–51]. The storage granules of PHA require other associated proteins to protect their hydrophobic core from the cytoplasm, all of which play a role in regulating the number and sizes of the granules produced. The most abundant granule-associated protein is an amphiphilic protein known as phasin (PhaP) [52].

The over-expression of proteins involved in this storage mechanism in strain Cad16^T, such as the PhaE subunit of PHA synthase and phasins (PhaP), suggested the presence of sufficient amounts of both carbon sources and reducing factors in the cells during the light period, likely originating from photosynthesis [53]. This storage mechanism is commonly observed in phototrophic and chemotrophic bacteria [54].

3.2.3. *Sulfur compound oxidation and photosynthesis*

Purple sulfur bacteria can grow photo-autotrophically using inorganically reduced sulfur compounds (i.e. S^{-2}, S^0 and $S_2O_3^{2-}$) as electron donors for CO_2 fixation via the CBB cycle [11]. The photochemical reaction centre complex uses light energy to transfer electrons from reduced sulfur compound to $NAD(P)^+$ [55]. Dissimilatory sulfite reductase (DsrAB, a tetramer composed of two alpha and two beta subunits) is responsible for the oxidation of the sulfide (S^{-2}) to sulfite (SO_3^{2-}) to generate electrons for photosynthetic CO_2 reduction. This enzyme is also required for the oxidation of intracellularly stored sulfur granules, especially in sulfur-storing PSB [56]. DsrAB has been reported to bind another subunit, called gamma subunit DsrC [57,58]. This gamma subunit (DsrC) was more abundant in our organism during the light period (Table 2, spot L20), suggesting an over-expression of the dissimilatory sulfite reductase enzyme.

The photosynthetic reaction centre (PSI) is also responsible for generating the proton motive force necessary for ATP generation by the ATP synthase. The ATP synthase subunit alpha (spot L4) was more abundant in the light. This ubiquitous enzyme is present in the plasma membrane of bacteria, the thylakoid membrane of chloroplasts, and the inner mitochondrial membrane. ATP synthase is a transmembrane protein, and for this reason it is composed of two distinct regions: the hydrophobic F_0, which is embedded in the membrane and allows the transit of protons, and the hydrophilic F_1, a complex composed of five types of subunits: $\alpha 3$ (Table 2, spot L4), $\beta 3$, $\gamma 1$, $\delta 1$ and $\varepsilon 1$ [59]. At low activity of the proton motive force, the flow is reversed, and the enzyme functions as a proton-pumping ATPase. In many bacterial species (mostly anaerobic), the reverse reaction is essential for life, when neither the respiratory chain nor the photosynthetic proteins are able to generate the proton motive force. In this way, many important cellular functions, such as flagellar motility or ion\nutrient transmembrane transport are supported.

The photosynthetic lifestyle of the PSB from Lake Cadagno and especially of *Candidatus* "T. syntrophicum" strain Cad16^T, was previously investigated [13,14,16–18]. We were therefore surprised to find a relatively low number of expressed proteins related to photosynthesis, such as RuBisCO. It is known that many bacteria have microcompartments that concentrate the metabolically related enzymes to increase their efficiency and to control the flow and concentrations of substrates and intermediates [60,61]. During the CO_2-fixing process, different phototrophic bacteria showed the presence of carboxysome-like microcompartments that encapsulate RuBisCO and carbonic anhydrase and thereby enhance carbon fixation by increasing the levels of CO_2 in the vicinity of RuBisCO [62,63]. All the genes that are involved in the formation of a carboxysome-like microcompartment are present immediately after the type I RuBisCO *cbbL* and *cbbS* genes in the draft genome of strain Cad16^T (Genbank: JQ693375–JQ693380). In our analysis, these large, complex carboxysome shell structures could be lost during the extraction of the total proteins or during the protein separation process, and for this reason, we did not observe the type I RuBisCO (CbbL or CbbS) in our gels. However, by our results the simply explanation was the absence of relevant difference in the expression between the light and the dark condition of these proteins.

3.2.4. *Transmembrane transport proteins*

Additional proteins that showed strong expression in *Candidatus* "T. syntrophicum" strain Cad16^T in the presence of light were those involved in transmembrane transport, such as unspecific porins (Table 2, spots L3, L5 and L6) and more specifically, ABC transporter (Table 2, spots L10 and L11). Porins are proteins that cross cellular membranes in Gram-negative bacteria and act like a pore, through which different types of molecules up to 600 Da can diffuse. Their expression is regulated by the environmental conditions of growth. Porins allow cells to fine tune the uptake of appropriate nutrients and to protect themselves optimally against external factors, such as osmotic pressure and temperature [64]. ABC transporters are transmembrane proteins that utilise energy from the hydrolysis of ATP to transport various substrates across the membrane. Proteins are classified as ABC transporters based on the sequence and organisation of their ATP-binding cassette (ABC) domain(s), and they are specific for the uptake of a large variety of nutrients, such as sugars, amino acids, peptides, inorganic ions and vitamins [65,66]. Moreover, it was shown that ABC transporters are important in the antibiotic resistance in different bacteria [67–69]. Many secondary metabolites (e.g. antibiotics and toxins) are toxic to the microorganisms that produce them, so ABC transporters would avoid inhibition of growth of the producing strain by preventing the drug from going back to the cell, acting as a one-way in-out pump.

The increased expression of the transmembrane transport proteins suggested a strong interaction between the cells and their environment for the uptake of nutriments and the excretion of metabolites.

3.2.5. *Other metabolic processes*

Other cellular metabolic processes were also highlighted while analysing the total proteins that were extracted from *Candidatus* "T. syntrophicum" strain Cad16^T in the presence of light. The methyl-accepting chemotaxis protein (MCP) (Table 2, spot L22), a component of the chemotactic response system in bacteria and archaea, governs the migration of bacteria towards chemical attractants and away from repellents by translating temporal changes in the levels of chemical stimuli into a modulation of the cell's swimming direction [70]. MCP is a transmembrane sensor protein in bacteria, allowing the detection of concentrations of molecules in the extracellular matrix [71]. *Candidatus* "T. syntrophicum" strain Cad16^T is highly metabolically active in the light and use this MCP to search for nutrients. It could be that the expression of this gene is an automatic reply to external stimuli, e.g. the need of substances involved in some metabolic pathways [72].

Moreover, five other spots more abundant in the presence of light (Table 2, spots L9, L12, L13, L16 and L19) were identified as "hypothetical proteins" or "Uncharacterised conserved protein". However, conserved domains were recognised in two of this spots (Table 2, spots L12 and L19) using BLASTp analysis (http://blast.ncbi.nlm.nih.gov/). Spot L12 showed a tellurium cassette component in its sequence. In the past, prior to the development of antibiotics, tellurite compounds were used

to treat conditions such as leprosy, tuberculosis, dermatitis, cystitis and eye infections. It has been proposed that tellurite toxicity is due to its strong oxidising ability and its ability to replace sulphur in various cellular functions [73]. An analysis of the protein spot L19 highlighted the presence of a SpoVT/AbrB-like domain. In *Bacillus subtilis*, this domain appears to be involved in the transcription activation of the repression of genes expressed during the transition state between the exponential and the stationary phase. Antibiotic resistance protein B (AbrB) is a representative of a large superfamily of known and putative transcription factors that includes transition-state regulators, putative regulators of cell wall biosynthesis, regulators of phosphate uptake, and a large number of proteins of as yet unknown activity [74]. However, we must be cautious and use this identification by BLASTp as a strictly hypothetical identification. Unfortunately, the hypothetical proteins of spots L9, L13 and L16 did not show any conserved domains in their gene sequence, and for this reason, their function remain unknown. These uncharacterised proteins and those showing a conserved domain were likely proteins with unknown functions, or they were not yet annotated in our draft genome (e.g. between 2 contigs).

3.3. *Protein spots more abundant in the dark*

Among the 17 protein spots that were more abundant in the dark, we found proteins that were mainly involved with (a) isomerases, (b) carbon dioxide fixation, (c) stress metabolism and (d) other metabolic processes.

3.3.1. *Isomerases*

The main proteins expressed by *Candidatus* "T. syntrophicum" strain Cad16^T in the dark belonged to the family of isomerases, especially to the peptidyl-prolyl isomerases (PPIs) and protein disulphide isomerase (PDI) (Table 2, spots D1, D2, D8, D9 and D12). PPIs promote proper protein folding by increasing the rate of transition of proline residues between the *cis* and *trans* states, and they also possess a chaperone-like activity. Proteins with prolyl isomerase activity include cyclophilin, FKBPs, and parvulin, although larger proteins can also contain prolyl isomerase domains [75]. PDI is an enzyme that catalyses the formation and breakage of disulphide bonds via its four thioredoxin-like domains. PDI can act also as a chaperone by assisting in the reactivation of denatured proteins that do not contain cysteine residues. In *E. coli*, 2 prologue proteins of PDI (DsbC and DsbG) are located in the periplasmic space outside the cytoplasm [76].

It is difficult to interpret the considerable number of isomerases that were more abundant in the dark; however, they could play a certain chaperone role through the use of the stored substances produced during the phototrophic activity in the light.

3.3.2. *Carbon dioxide fixation*

The ability of *Candidatus* "T. syntrophicum" strain Cad16^T to fix CO_2 in the dark was previously observed in several others experimental analyses; however, the mechanism involved in the dark assimilation is not yet understood [15,17]. We found three protein spots that were more abundant in the dark (Table 2, spots D5, D6 and D11) and were identified as components involved in different pathways of CO_2 fixation [9]. The first enzyme, the malate dehydrogenase (MDH) (Table 2, spot D6), is an enzyme part of the reverse tricarboxylic acid (rTCA) cycle found especially in anaerobic bacteria (e.g. GSB) and of the dicarboxylate/4-hydroxybutyrate (DC/HB) cycle found at the present day only in some archaeal species [77,78]. This enzyme reversibly reduces the oxaloacetate in malate using the oxidation of NADH to NAD^+. Interestingly, also the others two enzymes up-regulated in the dark could be part of the DC/HB cycle, catalysing the 2 last reactions of the cycle: the oxidation of 3-hydroxybutyryl-CoA in acetoacetyl-CoA using $NAD(P)^+$ as an electron acceptor catalyses by the enzyme 3-hydroxyacyl-CoA dehydrogenase (Table 2, spot D11), and the oxidisation of acetoacetyl-CoA in 2 acetyl-CoA catalyses by the enzyme acetyl-CoA acetyltransferase (Table 2, spot D5). However, these two enzymes could also be part of the last step of the beta-oxidation of fatty acid and PHB granules. The degradation of the PHB granules produced during the day in the presence of light (see the Section 3.2.2 before) might produce acetyl-CoA and reducing power in the form of NAD(P)H. Both substrates are potentially used in the CO_2 fixing process (rTCA or/and DC/HB cycle or others) during the dark period. Therefore, the rTCA or the DC/HB cycle have to be investigated more in the detail in strain Cad16^T.

3.3.3. *Stress metabolism*

Proteins involved in the oxidative stress response (superoxide and hydrogen peroxide) were also detected (Table 2, spots D13, D14 and D16). Superoxide dismutase is an enzyme that catalyses the dismutation of superoxide into oxygen and hydrogen peroxide. It plays an important antioxidative role in cells that are exposed to oxygen. Peroxiredoxins are a ubiquitous family of antioxidant enzymes that use thioredoxin (Trx) to detoxify hydrogen peroxide. Moreover, these types of proteins can also act as molecular chaperones and, most importantly, as regulators in the 24 h internal circadian clock of many organisms [79–81]. *Candidatus* "T. syntrophicum" strain Cad16^T was grown in autotrophic Pfennig's medium (see Section 2) without the presence of oxygen in the gas phase; therefore, the up-regulation of these proteins, especially peroxiredoxin, could be linked to the circadian rhythm mechanism. Indeed, the cellular ROS balance is important for robust 24 h circadian clock function, as was recently described in *Neurospora* [82].

Another possible explanation for these anti-stress enzymes comes from one of the key enzymes of the DC/HB cycle. In fact, the 4-hydroxybutyryl-CoA dehydratase is considered a "radical enzyme" that uses radicals as intermediates and enables the metabolism of otherwise refractory compounds. Because they are highly reactive towards dioxygen, radicals are often found during catalysis by enzymes from anaerobic microorganisms [83–85]. An hypothetical enhanced activity of 4-hydroxybutyryl-CoA dehydratase in the dark most likely produced more dangerous free radicals, which were limited by the simultaneous increased expression of antioxidant enzymes.

3.3.4. *Other metabolisms*

Similar to what was observed from proteins that were more abundant in the light, we also found a membrane transport mechanism that was highlighted in the dark. A maltose ABC

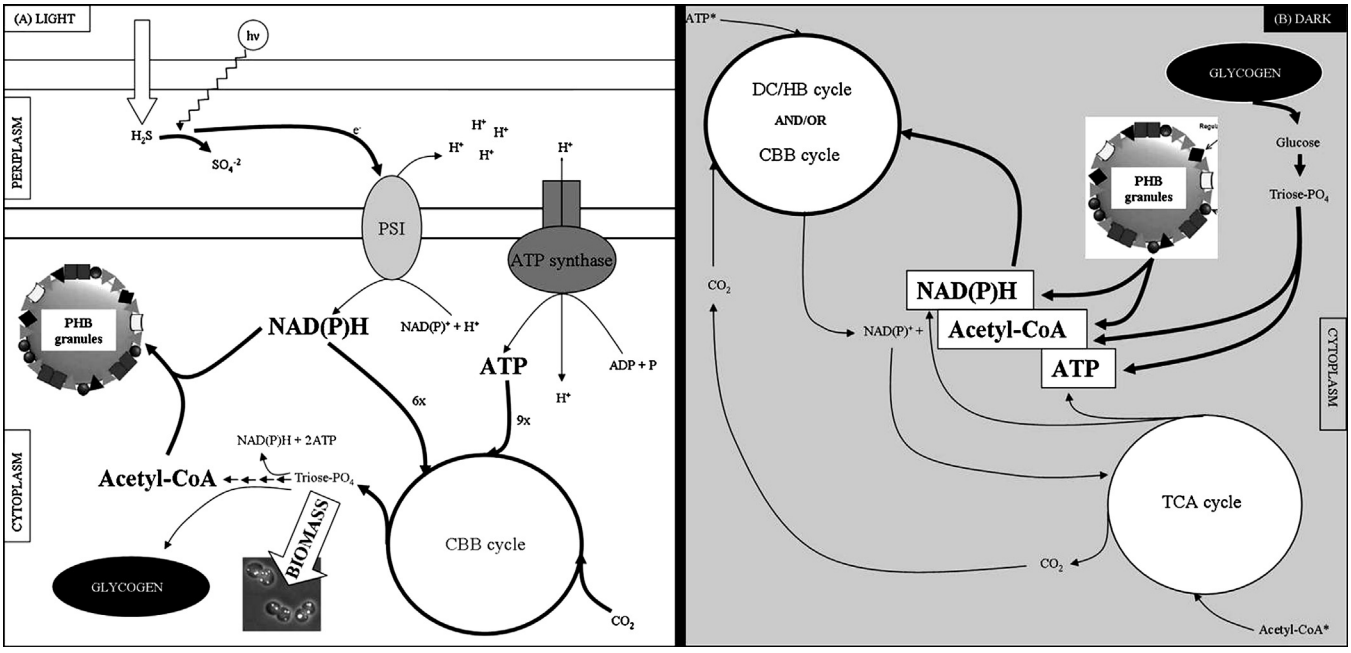

Fig. 2 – Scheme summarising the majors metabolic pathways suggested from 2D-DIGE analysis, (A) in presence of light and (B) in the dark.

transporter periplasmic protein (Table 2, spot D4) was found to be more abundant during the dark phase.

Moreover, 5 protein spots that were more abundant in the dark (Table 2, spots D3, D7, D10, D15 and D17) were identified as "hypothetical proteins". Unfortunately, no conserved domains were found after online pBLAST analysis for four of the five spots. A specific domain was assigned only to spot D15, which identified tellurite resistance from the domain, similar to the protein spot L12 that was also more abundant in the light.

3.4. *Proteins with unvaried abundance*

Protein spots with similar expression level between the light/dark conditions were also analyses. From the 13 selected spots (see Table 2; N1–N13), we found important housekeeping proteins, such as ribosomal proteins and periplasmic glucan biosynthesis proteins (Table 2, spots N1, N12 and N13). Interesting proteins potentially involved in the stress metabolism (Table 2, spots N9 and N10) or implicated in other cellular mechanisms such as the circadian rhythm (see Section 3.3.3) were also found. Furthermore, the presence of type II RuBisCO protein (Table 2, spot N3) in the unchanging expressed protein confirmed recent results that showed a constant expression of the *cbbM* gene throughout a day in strain Cad16^T [17].

4. Conclusion

We present here the first analysis of the expression changes in the proteome between the light and dark phases of a PSB grown in anoxic autotrophic conditions. Our goal was to investigate the mechanisms behind the high capacity of these bacteria, and especially of the PSB *Candidatus* "T. syntrophicum" strain Cad16^T, to assimilate inorganic carbon in the dark. While the mechanism of CO_2 fixation in the presence of light provided by the CBB cycle is relatively well known [86], the assimilation of inorganic carbon in the dark remains poorly understood. In this study, we showed that 3 enzymes that were more abundant in the dark could be part of the anaerobic dicarboxylate/4-hydroxybutyrate (DC/HB) cycle, which represents an autotrophic CO_2 fixation pathway that is found in some archaea [9]. The substrates needed for this process such as reducing power and energy could be provided by the degradation of the storage globules of poly(3-hydroxybutyrate) (PHB), which synthesis was shown to be more abundant during the light conditions. In conclusion, the abundant presence of enzymes potentially involved in the autotrophic DC/HB cycle in the dark suggests to us a possible explanation for the high capacity shown by PSB, and especially in strain Cad16^T, to fix CO_2 in the absence of light. In the future we will try to learn more about the effective capacity of strain Cad16^T to fix CO_2 via this cycle. The scheme of Fig. 2 summarise the majors metabolic reactions in presence of light (Fig. 2A) or in the dark (Fig. 2B).

Acknowledgments

Financial support for this project was provided by the University of Geneva, the Institute of Microbiology and State of Ticino, and the Swiss National Science Foundation (grant no. 31003A-116591). The authors are indebted to Cinzia Benagli, Sophie De Respinis and Natalia Giot for technical and moral support. Furthermore, we are grateful to D. Burri and M. Wittwer from SPIEZ Laboratory, Federal Office for Civil Protection (FOCP), Spiez (Switzerland), for their technical support. The authors would also like to thank the FEMS and Alpine Biology Center Foundation (ABC) for their support.

REFERENCES

[1] Tonolla M, Demarta A, Peduzzi R, Hahn D. In situ analysis of phototrophic sulfur bacteria in the chemocline of meromictic Lake Cadagno (Switzerland). Applied and Environmental Microbiology 1999;65:1325–30.

[2] Decristophoris PMA, Peduzzi S, Ruggeri-Bernardi N, Hahn D, Tonolla M. Fine scale analysis of shifts in bacterial community structure in the chemocline of meromictic Lake Cadagno, Switzerland. Journal of Limnology 2009;68:16–24.

[3] Tonolla M, Peduzzi R, Hahn D. Long-term population dynamics of phototrophic sulfur bacteria in the chemocline of Lake Cadagno, Switzerland. Applied and Environmental Microbiology 2005;71:3544–50.

[4] Imhoff JF. Bergey's manual of systematic bacteriology. Springer; 2005.

[5] Van Gemerden H, Mas J. Ecology of phototrophic sulfur bacteria. Boston: Kluwer Academic Publishers (Springer); 2004.

[6] Frigaard N-U, Bryant D. Chlorosomes: antenna organelles in photosynthetic green bacteria. Complex Intracellular Structures in Prokaryotes 2006;7:9–114.

[7] Tang JK-H, Saikin SK, Pingali SV, Enriquez MM, Huh J, Frank HA, et al. Temperature and carbon assimilation regulate the chlorosome biogenesis in green sulfur bacteria. Biophysical Journal 2013;105:1346–56.

[8] Law CJ, Roszak AW, Southall J, Gardiner AT, Isaacs NW, Cogdell RJ. The structure and function of bacterial light-harvesting complexes (review). Molecular Membrane Biology 2004;21:183–91.

[9] Berg IA. Ecological aspects of the distribution of different autotrophic CO_2 fixation pathways. Applied and Environmental Microbiology 2011;77:1925–36.

[10] Sirevag R, Buchanan BB, Berry JA, Troughton JH. Mechanisms of CO_2 fixation in bacterial photosynthesis studied by the carbon isotope fractionation technique. Archives of Microbiology 1977;112:35–8.

[11] Frigaard NU, Dahl C. Sulfur metabolism in phototrophic sulfur bacteria. London: Academic Press; 2009.

[12] Overmann J. Sulfur metabolism in phototrophic organisms: ecology of phototrophic sulfur bacteria. Urbana: Springer; 2008.

[13] Camacho A, Erez J, Chicote A, Florin M, Squires M, Lehmann C, et al. Microbial microstratification, inorganic carbon photoassimilation and dark carbon fixation at the chemocline of the meromictic Lake Cadagno (Switzerland) and its relevance to the food web. Aquatic Sciences 2001;63:91–106.

[14] Casamayor EO, Garcia-Cantizano J, Pedros-Alio C. Carbon dioxide fixation in the dark by photosynthetic bacteria in sulfide-rich stratified lakes with oxic-anoxic interfaces. Limnology and Oceanography 2008;53:1193–203.

[15] Casamayor EO, Lliros M, Picazo A, Barberan A, Borrego CM, Camacho A. Contribution of deep dark fixation processes to overall CO_2 incorporation and large vertical changes of microbial populations in stratified Karstic lakes. Aquatic Sciences – Research Across Boundaries 2012;74:61–75.

[16] Musat N, Halm H, Winterholler B, Hoppe P, Peduzzi S, Hillion F, et al. A single-cell view on the ecophysiology of anaerobic phototrophic bacteria. Proceedings of the National Academy of Sciences 2008;105:17861–6.

[17] Storelli N, Peduzzi S, Saad MM, Frigaard NU, Perret X, Tonolla M. CO_2 assimilation in the chemocline of Lake Cadagno is dominated by a few types of phototrophic purple sulfur bacteria. FEMS Microbiology Ecology 2013;84:421–32.

[18] Peduzzi S, Storelli N, Welsh A, Peduzzi R, Hahn D, Perret X, et al. *Candidatus* Thiodictyon syntrophicum, sp. nov., a new purple sulfur bacterium isolated from the chemocline of Lake Cadagno forming aggregates and specific associations with *Desulfocapsa* sp. Systematic and Applied Microbiology 2012;35:139–44.

[19] Arioli S, Roncada P, Salzano AM, Deriu F, Corona S, Guglielmetti S, et al. The relevance of carbon dioxide metabolism in *Streptococcus thermophilus*. Microbiology 2009;155:1953–65.

[20] Kluge S, Hoffmann M, Benndorf D, Rapp E, Reichl U. Proteomic tracking and analysis of a bacterial mixed culture. Proteomics 2012;12:1893–901.

[21] Tannu NS, Hemby SE. Two-dimensional fluorescence difference gel electrophoresis for comparative proteomics profiling. Nature Protocols 2006;1:1732–42.

[22] Tomanek L. Environmental proteomics: changes in the proteome of marine organisms in response to environmental stress, pollutants, infection, symbiosis, and development. Annual Review of Marine Science 2011;3:373–99.

[23] Yonemori H, Kubota D, Taniguchi H, Tsuda H, Fujita S, Murakami Y, et al. Laser microdissection and two-dimensional difference gel electrophoresis with alkaline isoelectric point immobiline gel reveals proteomic intra-tumor heterogeneity in colorectal cancer. EuPA Open Proteomics 2013;1:17–29.

[24] Görg A, Weiss W, Dunn MJ. Current two-dimensional electrophoresis technology for proteomics. Proteomics 2004;4:3665–85.

[25] O'Farrell PH. High resolution two-dimensional electrophoresis of proteins. Journal of Biological Chemistry 1975;250:4007–21.

[26] Marouga R, David S, Hawkins E. The development of the DIGE system: 2D fluorescence difference gel analysis technology. Analytical and Bioanalytical Chemistry 2005;382:669–78.

[27] Alban A, David SO, Bjorkesten L, Andersson C, Sloge E, Lewis S, et al. A novel experimental design for comparative two-dimensional gel analysis: two-dimensional difference gel electrophoresis incorporating a pooled internal standard. Proteomics 2003;3:36–44.

[28] Pappin DJ, Hojrup P, Bleasby AJ. Rapid identification of proteins by peptide-mass fingerprinting. Current Biology: CB 1993;3:327–32.

[29] Henzel WJ, Billeci TM, Stults JT, Wong SC, Grimley C, Watanabe C. Identifying proteins from two-dimensional gels by molecular mass searching of peptide fragments in protein sequence databases. Proceedings of the National Academy of Sciences 1993;90:5011–5.

[30] Eichler B, Pfennig N. A new purple sulfur bacterium from stratified freshwater lakes, *Amoebobacter purpureus* sp. nov. Archives of Microbiology 1988;149:395–400.

[31] Widdel F, Bak F. Gram-negative mesophilic sulfate-reducing bacteria. The Prokaryotes 1992;4:3352–78.

[32] Hobbie JE, Daley RJ, Jasper S. Use of nuclepore filters for counting bacteria by fluorescence microscopy. Applied and Environmental Microbiology 1977;33:1225–8.

[33] Bradford MM. A rapid and sensitive method for the quantitation of microgram quantities of protein utilizing the principle of protein-dye binding. Analytical Biochemistry 1976;72:248–54.

[34] Karp NA, Lilley KS. Maximising sensitivity for detecting changes in protein expression: experimental design using minimal CyDyes. Proteomics 2005;5:3105–15.

[35] Syrovy I, Hodny Z. Staining and quantification of proteins separated by polyacrylamide gel electrophoresis. Journal of Chromatography B: Biomedical Sciences and Applications 1991;569:175–96.

[36] Perkins DN, Pappin DJ, Creasy DM, Cottrell JS. Probability-based protein identification by searching sequence databases using mass spectrometry data. Electrophoresis 1999;20:3551–67.
[37] Wang Z, Gerstein M, Snyder M. RNA-Seq: a revolutionary tool for transcriptomics. Nature Reviews Genetics 2009;10:57–63.
[38] Richardson JP. Rho-dependent termination and ATPases in transcript termination. Biochimica et Biophysica Acta-Gene Structure and Expression 2002;1577:251–60.
[39] Marintchev A, Wagner G. Translation initiation: structures, mechanisms and evolution. Quarterly Reviews of Biophysics 2004;37:197–284.
[40] Nissen P, Hansen J, Ban N, Moore PB, Steitz TA. The structural basis of ribosome activity in peptide bond synthesis. Science 2000;289:920–30.
[41] Helgstrand M, Mandava CS, Mulder FAA, Liljas A, Sanyal S, Akke M. The ribosomal stalk binds to translation factors IF2, EF-Tu, EF-G and RF3 via a conserved region of the L12 C-terminal domain. Journal of Molecular Biology 2007;365:468–79.
[42] Ganoza MC, Kiel MC, Aoki H. Evolutionary conservation of reactions in translation. Microbiology and Molecular Biology Reviews 2002;66:460–85.
[43] Hartl FU, Hayer-Hartl M. Molecular chaperones in the cytosol: from nascent chain to folded protein. Science 2002;295:1852–8.
[44] Sudesh K, Abe H, Doi Y. Synthesis, structure and properties of polyhydroxyalkanoates: biological polyesters. Progress in Polymer Science 2000;25:1503–55.
[45] Jendrossek D. Polyhydroxyalkanoate granules are complex subcellular organelles (carbonosomes). Journal of Bacteriology 2009;191:3195–202.
[46] Haywood GW, Anderson AJ, Chu L, Dawes EA. The role of NADH-and NADPH-linked acetoacetyl-CoA reductases in the poly-3-hydroxybutyrate synthesizing organism *Alcaligenes eutrophus*. FEMS Microbiology Letters 1988;52:259–64.
[47] Liebergesell M, Steinbüchel A. Cloning and nucleotide sequences of genes relevant for biosynthesis of poly (3-hydroxybutyric acid) in *Chromatium vinosum* strain D. European Journal of Biochemistry 1992;209:135–50.
[48] Liebergesell M, Steinbüchel A. Cloning and molecular analysis of the poly (3-hydroxybutyric acid) biosynthetic genes of *Thiocystis violacea*. Applied Microbiology and Biotechnology 1993;38:493–501.
[49] Fukui T, Shiomi N, Doi Y. Expression and characterization of (R)-specific enoyl coenzyme A hydratase involved in polyhydroxyalkanoate biosynthesis by *Aeromonas caviae*. Journal of Bacteriology 1998;180:667–73.
[50] Tsuge T, Fukui T, Matsusaki H, Taguchi S, Kobayashi G, Ishizaki A. Molecular cloning of two (R)-specific enoyl-CoA hydratase genes from *Pseudomonas aeruginosa* and their use for polyhydroxyalkanoate synthesis. FEMS Microbiology Letters 2006;184:193–8.
[51] Vo MT, Lee K-W, Jung Y-M, Lee Y-H. Comparative effect of overexpressed *phaJ* and *fabG* genes supplementing (*R*)-3-hydroxyalkanoate monomer units on biosynthesis of mcl-polyhydroxyalkanoate in *Pseudomonas putida* KCTC1639. Journal of Bioscience and Bioengineering 2008;106:95–8.
[52] Steinbüchel A, Aerts K, Liebergesell M, Wieczorek R, Babel W, Föllner C, et al. Considerations on the structure and biochemistry of bacterial polyhydroxyalkanoic acid inclusions. Canadian Journal of Microbiology 1995;41:94–105.
[53] Overmann J, Garcia-Pichel F. Prokaryotes the phototrophic way of life. Springer; 2006.
[54] Hazer DB, Kiliçay E, Poly Hazer B. (3-Hydroxyalkanoate)s: diversification and biomedical applications: a state of the art review. Materials Science and Engineering: C 2012;32:637–47.
[55] Brune D. Sulfur compounds as photosynthetic electron donors. Dordrecht/The Netherlands: Kluwer Academic Publishers; 1995.
[56] Pott AS, Dahl C. Sirohaem sulfite reductase and other proteins encoded by genes at the dsr locus of *Chromatium vinosum* are involved in the oxidation of intracellular sulfur. Microbiology 1998;144:1881–94.
[57] Cort JR, Selan U, Schulte A, Grimm F, Kennedy MA, Dahl C. *Allochromatium vinosum* DsrC: solution-state NMR structure, redox properties and interaction with DsrEFH, a protein essential for purple sulfur bacterial sulfur oxidation. Journal of Molecular Biology 2008;382:692–707.
[58] Pierik AJ, Duyvis MG, Helvoort JMLM, Wolbert RBG, Hagen WR. The third subunit of desulfoviridin-type dissimilatory sulfite reductases. European Journal of Biochemistry 2005;205:111–5.
[59] Feniouk BA, Suzuki T, Yoshida M. Regulatory interplay between proton motive force, ADP, phosphate, and subunit Ïμ in bacterial ATP synthase. Journal of Biological Chemistry 2007;282:764–72.
[60] Kerfeld CA, Sawaya MR, Tanaka S, Nguyen CV, Phillips M, Beeby M, et al. Protein structures forming the shell of primitive bacterial organelles. Science 2005;309:936–8.
[61] Yeates TO, Crowley CS, Tanaka S. Bacterial microcompartment organelles: protein shell structure and evolution. Annual Review of Biophysics 2010;39:185.
[62] Cannon GC, Heinhorst S, Kerfeld CA. Carboxysomal carbonic anhydrases: structure and role in microbial CO_2 fixation. Biochimica et Biophysica Acta (BBA)-Proteins & Proteomics 2010;1804:382–92.
[63] Yeates TO, Kerfeld CA, Heinhorst S, Cannon GC, Shively JM. Protein-based organelles in bacteria: carboxysomes and related microcompartments. Nature Reviews Microbiology 2008;6:681–91.
[64] Schulz GE. Bacterial porins: structure and function. Current Opinion in Cell Biology 1993;5:701–7.
[65] Davidson AL, Dassa E, Orelle C, Chen J. Structure, function, and evolution of bacterial ATP-binding cassette systems. Microbiology and Molecular Biology Reviews 2008;72:317–64.
[66] Moussatova A, Kandt C, O'Mara ML, Tieleman DP. ATP-binding cassette transporters in *Escherichia coli*. Biochimica et Biophysica Acta (BBA)-Biomembranes 2008;1778:1757–71.
[67] Méndez C, Salas JA. The role of ABC transporters in antibiotic-producing organisms: drug secretion and resistance mechanisms. Research in Microbiology 2001;152:341–50.
[68] Otto M, Götz F. ABC transporters of staphylococci. Research in Microbiology 2001;152:351–6.
[69] Martin JF, Casqueiro J, Liras P. Secretion systems for secondary metabolites: how producer cells send out messages of intercellular communication. Current Opinion in Microbiology 2005;8:282–93.
[70] Alon U, Surette MG, Barkai N, Leibler S. Robustness in bacterial chemotaxis. Nature 1999;397:168–71.
[71] Gestwicki JE, Lamanna AC, Harshey RM, McCarter LL, Kiessling LL, Adler J. Evolutionary conservation of methyl-accepting chemotaxis protein location in bacteria and archaea. Journal of Bacteriology 2000;182:6499–502.
[72] Martinez-Antonio A, Collado-Vides J. Identifying global regulators in transcriptional regulatory networks in bacteria. Current Opinion in Microbiology 2003;6:482–9.
[73] Taylor DE. Bacterial tellurite resistance. Trends in Microbiology 1999;7:111–5.
[74] Phillips ZEV, Strauch MA. *Bacillus subtilis* sporulation and stationary phase gene expression. Cellular and Molecular Life Sciences 2002;59:392–402.

[75] Fanghänel J, Fischer G. Insights into the catalytic mechanism of peptidyl prolyl cis/trans isomerases. Frontiers in Bioscience 2004;9:3453–78.
[76] Kadokura H, Katzen F, Beckwith J. Protein disulfide bond formation in prokaryotes. Annual Review of Biochemistry 2003;72:111–35.
[77] Huber H, Gallenberger M, Jahn U, Eylert E, Berg IA, Kockelkorn D, et al. A dicarboxylate/4-hydroxybutyrate autotrophic carbon assimilation cycle in the hyperthermophilic Archaeum *Ignicoccus hospitalis*. Proceedings of the National Academy of Sciences 2008;105:7851–6.
[78] Tang K-H, Tang YJ, Blankenship RE. Carbon metabolic pathways in phototrophic bacteria and their broader evolutionary implications. Frontiers in Microbiology 2011;2:1–23.
[79] Jang HH, Lee KO, Chi YH, Jung BG, Park SK, Park JH, et al. Two enzymes in one: two yeast peroxiredoxins display oxidative stress-dependent switching from a peroxidase to a molecular chaperone function. Cell 2004;117: 625–35.
[80] Knoops B, Loumaye E, Eecken V. Peroxiredoxin systems evolution of the peroxiredoxins. Netherlands: Springer; 2007.
[81] Edgar RS, Green EW, Zhao Y, van Ooijen G, Olmedo M, Qin X, et al. Peroxiredoxins are conserved markers of circadian rhythms. Nature 2012;485:459–64.
[82] Yoshida Y, Iigusa H, Wang N, Hasunuma K. Cross-talk between the cellular redox state and the circadian system in Neurospora. PloS one 2011;6:e28227.
[83] Buckel W, Golding BT. Radical species in the catalytic pathways of enzymes from anaerobes. FEMS Microbiology Reviews 1998;22:523–41.
[84] Buckel W, Golding BT. Radical enzymes in anaerobes. Annual Review of Microbiology 2006;60:27–49.
[85] Matias PM, Pereira IAC, Soares CM, Carrondo MA. Sulphate respiration from hydrogen in *Desulfovibrio bacteria*: a structural biology overview. Progress in Biophysics and Molecular Biology 2005;89:292–329.
[86] Tabita FR, Hanson TE, Li H, Satagopan S, Singh J, Chan S. Function, structure, and evolution of the RubisCO-like proteins and their RubisCO homologs. Microbiology and Molecular Biology Reviews 2007;71:576.